Available online at www.sciencedirect.com
ScienceDirect
Mendeleev Commun., 2017, **27**, 183–185
Mendeleev Communications

Electron transport and morphological changes in the electrode/erythrocyte system

Aslan Yu. Tsivadze,[a] Mogely Sh. Khubutiya,[b] Irina V. Goroncharovskaya,[b] Anatoly K. Evseev,[b] Michael M. Goldin,[c] Natalia V. Borovkova,[b] Oleg V. Batishchev[a] and Mark M. Goldin*[b]

[a] *A. N. Frumkin Institute of Physical Chemistry and Electrochemistry, Russian Academy of Sciences, 119071 Moscow, Russian Federation*
[b] *N. V. Sklifosovsky Research Institute of Emergency Medicine, 129090 Moscow, Russian Federation. E-mail: markmgold@gmail.com*
[c] *Oakland Community College, Bloomfield Hills, MI 48304, USA*

DOI: 10.1016/j.mencom.2017.03.026

Electrochemical interactions in the electrode/erythrocyte system leading to electron transport and morphological changes in erythrocyte depending on electrode potential were revealed.

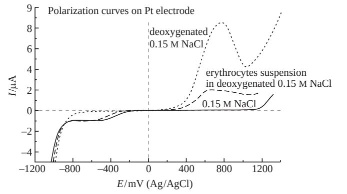

Blood cells possess an electric double layer due to a negative charge on their membrane surface,[1] which imparts an electrochemical character to interactions between blood cells and other materials that possess a surface electric charge. Moreover, the normal function of blood cells is related to the stability of charge density on cell membranes.[2–4] Therefore, it is hardly surprising that further elucidation of the mechanism of blood cell function has long involved the use of electrochemical criteria and models.

For instance, in a study of thrombosis, Sawyer[5,6] correlated the behavior of thrombocytes (platelets) with the charge on the surface of vascular walls or foreign material involved and proposed a fundamental hypothesis regarding charge transfer between the vascular walls or foreign material and blood cells. However, this hypothesis remains unverified.

On the other hand, the existence of electron transport across bacterial membranes has been confirmed by various investigators.[7–10] The mechanism of electron transport and, subsequently, the development of microbial fuel cells have been considered. However, the electrochemical activity of bacteria (*e.g.*, *Shewanella putrefacient* or *Geobacter sulfurreducens*) is due to fermentation processes involving cytochrome *c*[8] with the latter accumulating electrons on the outer membrane; these electrons can then be donated to potential acceptors (electrophiles) present in the media surrounding the bacterial cells. Note that this electron transport does not cause changes in the cell membrane. Furthermore, in the electrochemical activity of bacteria, electron transport is strictly unidirectional: electrons are transported from the outer cell membrane to extracellular electron acceptors.[7–10]

The above fermentation processes can also occur in blood cells; however, they are intercellular and hence cannot give rise to spontaneous directional electron transport into extracellular media. To activate the above electron transport across blood cell membranes, a potential gradient between the membrane and the extracellular media is required.

However, transmembrane electrochemistry problems are beyond the scope of this paper, and we will focus on electron transport between the electrode and the erythrocyte membrane surface.

To elucidate the interaction between the charged surface and the cell membrane, direct electrochemical measurements in the system of an electrode and suspended blood cells are needed. The use of erythrocytes as a model blood cell can be rationalized based on their relative stability in the presence of external forces, their longevity, and their natural coloring that renders staining for morphometry purposes unnecessary. Suitable electrode materials for such an investigation include a platinum electrode due to its traditional use as the electrode of choice in polarization measurements, and optically transparent materials deposited on glass, such as indium tin oxide (ITO) films, to enable optical observation of cell morphology depending on electrode polarization.†

In order to investigate the electrochemical behavior of erythrocytes at the platinum electrode, it was necessary to identify the range of potentials of a so-called double layer region where

---

† A physiologic saline solution (aqueous 0.15 м NaCl) was used as a supporting electrolyte. Packed red blood cells for preparing experimental erythrocyte suspensions were obtained with N.V. Sklifosovsky Research Institute of Emergency Medicine Institutional Review Board approval from whole blood of consenting adult volunteers by centrifugation using a 3.12R centrifuge (Jouan, France) at 4–6 °C and 1500*g* with the subsequent washing with physiologic saline to remove residual blood plasma. Erythrocyte counts in suspensions used in the electrochemical cell were 4.0×10^{12} cells dm^{-3} and 8.0×10^{9} cells dm^{-3} for the platinum electrode and the ITO electrode, respectively.

The polarization and microcoulometric measurements were performed with an IPC Pro L potentiostat (ZAO Kronas, Russia) in a three-electrode cell with the cathodic and anodic chambers divided by a polypropylene membrane. A platinum point electrode and platinum wire mesh were used as working and auxiliary electrodes, respectively. Potentials were measured against a saturated silver/silver chloride reference electrode.

For microcoulometric measurements, the electrochemical cell was filled with a supporting electrolyte, and the platinum electrode was polarized to a set potential for 30 min; subsequently, the erythrocyte suspension was added to the electrolyte, and microcoulometric data were collected for 30 min.

Oxygen was removed from the supporting electrolyte by the addition of Na_2SO_3 to a final concentration of 0.02 м in the electrochemical cell, and its amount was monitored in the cell *via* a sulfite anode oxidation peak. The morphometry of stained cell preparations[12] was used to check electrooxidation and electroreduction did not occur in the supporting electrolyte. Indeed, one might expect the occurrence of certain processes at the platinum electrode in 0.15 M aqueous NaCl, such as the electroreduction of dissolved oxygen in the cathodic potential range, possibly synthesizing chemically active species in solution capable of damaging blood cells (*e.g.*, active oxygen species such as H_2O_2, $HO^{-\bullet}$ radical anions or similar unstable oxidizers formed in the course of dissolved oxygen electroreduction[11]).

Indeed, a peak wave with the half-wave potential corresponding to oxygen electroreduction was observed at –340 mV (Figure 1, curve *1*). To minimize the above electrochemical processes, aqueous sodium sulfite was added to the supporting electrolyte. The data in Figure 1 (curve *2*) showed the absence of an oxygen electroreduction peak wave in the deoxygenated supporting electrolyte. The addition of suspended erythrocytes to the deoxygenated supporting electrolyte led to the appearance of a reduction peak wave with a half-wave potential of –420 mV (Figure 1, curve *3*). The observed difference in the half-wave potentials indicates that the reduction processes in the supporting electrolyte with dissolved oxygen and with deoxygenated erythrocyte suspension can be attributed to different processes. It was also shown that the addition of a deoxygenating agent (sodium sulfite) into the supporting electrolyte led to an increase in the current observed for anodic potentials above +250 mV in both the solution (Figure 1, curve *2*) and the erythrocyte suspension (Figure 1, curve *3*). This effect corroborated the presence of a residual deoxygenating agent in both the supporting electrolyte and in the presence of suspended erythrocytes. The decrease in the sulfite electrooxidation peak height after the addition of erythrocytes to the electrolyte (curve *3*) compared to the pure deoxygenated supporting electrolyte (curve *2*) indicates the consumption of sulfite to compensate for the additional oxygen eluting from the erythrocytes. The presence of a sodium sulfite oxidation peak (*i.e.*, the presence of unreacted sulfite for 30 min) in the presence of erythrocytes definitely proves the absence of oxygen from the system during the measurement.

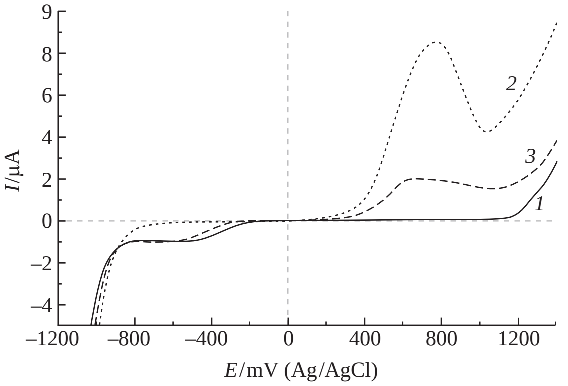

Figure 1 Polarization curves at the platinum electrode: (*1*) supporting electrolyte with dissolved oxygen, (*2*) deoxygenated supporting electrolyte with 0.02 M Na_2SO_3, and (*3*) deoxygenated supporting electrolyte with 0.02 M Na_2SO_3 containing suspended erythrocytes. Scan rate, 10 mV s^{-1}.

Thus, a reduction peak wave observed in the deoxygenated erythrocyte suspension provides direct evidence for electron transport between the electrode and erythrocyte membranes; it can be rationalized as the electroreduction of electron acceptor functional groups on the membrane surface.

However, anodic processes were not observed in the absence of sodium sulfite from the supporting electrolyte up to a potential of +1100 mV. In order to determine whether a method with increased sensitivity may help to detect anodic oxidation in an erythrocyte suspension, microcoulometry was used to investigate the [electrode]/[erythrocyte] system. According to the microcoulometry data, the charge Q needed to maintain a constant potential of the platinum electrode in the supporting electrolyte (Q_1) and in the erythrocyte suspension (Q_2) varied considerably. The difference between these charges ($\Delta Q = Q_1 - Q_2$) depended upon the applied electrode potential (Figure 2).

Thus, anodic oxidation in the presence of suspended erythrocytes at potentials greater (more positive) than +200 mV was observed, directly corroborating the occurrence of electron transport between the electrode and erythrocytes at anodic electrode potentials. The data also confirmed the occurrence of cathodic reduction in the presence of suspended erythrocytes in a potential range below (more negative than) –150 mV.

Erythrocyte morphometry data were obtained at the optically transparent electrode ITO in a potential range from –400 to +1400 mV (Figure 3). According to Figure 3, the initial normal morphology (discocytes) degenerates into various pathological morphologies with changes in electrode potential. Importantly, each of the morphologies occurred in a specific potential range. For instance, all discocytes transform into echinocytes at potentials more negative than –300 mV. With increasingly negative potentials below this value, the entire sample of red blood cells gradually takes on a spherocyte morphology.

For anodic potentials up to +600 mV, no changes in cell morphologies were detected. However, a very important effect was observed at potentials between +600 and +1200 mV, where the degenerative erythrocyte forms (echinocyte) changed back to the normal discocytes. Finally, for potentials more positive than +1300 mV, normal discocytes transferred into a different pathological form (stomatocytes).

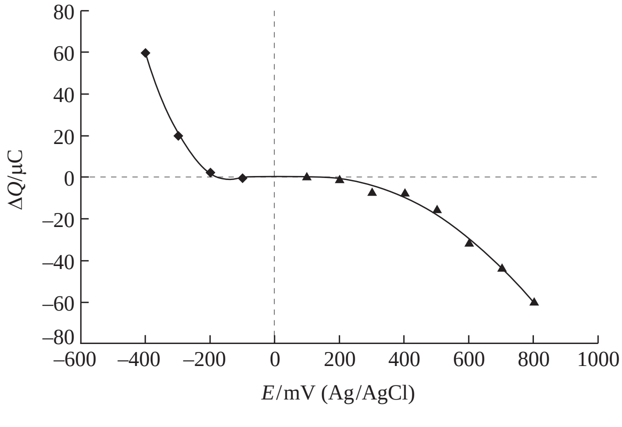

Figure 2 Microcoulometry measurements in the platinum electrode/erythrocyte system depending on electrode potential.

---

for changes in erythrocytes after contact with sodium sulfite. This test was carried out 30 min after the initial erythrocyte suspension was mixed with the supporting electrolyte containing 0.02 M Na_2SO_3. The absence of morphological changes after 30 min of contact with sodium sulfite in solution corroborates the hypothesis that erythrocytes are not affected by the small amounts of Na_2SO_3 in the supporting electrolyte.

The use of optically transparent ITO electrodes enabled the use of light microscopy to detect real-time morphological changes in erythrocytes depending on the applied electrode potential. A three-electrode cell was used for this purpose, where the ITO electrode (28.3 mm^2) formed the bottom portion of the cell, and a carbon black electrode was an auxiliary electrode. An Eclipse TS100 inverted light microscope (Nikon, Japan) with a CFI Achromat LWD 40×/0.55 objective lens (Nikon, Japan) was used to observe the morphologies of erythrocytes.

Erythrocytes concentration was detected by the Ac*T Diff2 hematology analyzer (Beckman Coulter, USA). Current–potential relationships were obtained by linear potential sweep from 0.0 to –1100 mV (cathodic curves) and from 0.0 to +1400 mV (anodic curves). Experiments with erythrocytes were performed in an anode potential region without sulfite adding into electrolyte; therefore, the excess of sodium sulfite was determined for experiments in the cathodic region only.

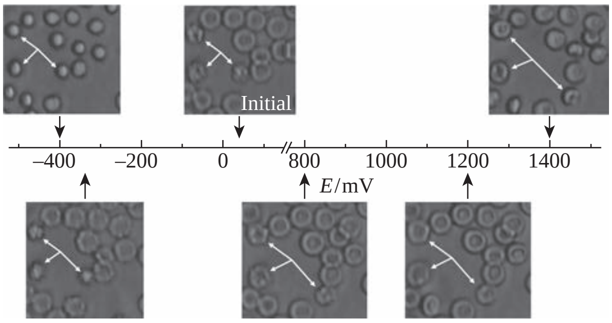

Figure 3 Changes in discocyte morphology with a linear potential sweep at the ITO electrode. Scan rate, 10 mV s^{-1}. Embedded microphotographs at a 400× magnification with arrows identifying three echinocytes in the initial sample and their morphological changes corresponding to different potentials.

Irreversible damage, leading to the disappearance of a portion of erythrocytes from the field of view, occurs at potentials more positive than +1300 mV or more negative than –350 mV. This can be caused by blood cells experiencing the electrical breakdown of their membranes followed by the desorption of the broken-down blood cells.

Thus, we experimentally confirmed the existence of electron transport between the electrode and erythrocytes. A correlation between the electrode potential and the morphologies of red blood cells was established with both reversible and irreversible potential-dependent morphologic changes. The observed effects are useful in the development of diagnostic methods for erythrocyte quality control and, possibly, methods for improving their quality when storage is prolonged by electrode polarization to given potential ranges.

References

1 Y. Yawata, *Cell Membrane: The Red Blood Cell as a Model*, Wiley-VCH, Weinheim, 2003.
2 M. M. Goldin, A. G. Volkov, Y. S. Goldfarb and M. M. Goldin, *J. Electrochem. Soc.*, 2006, **153**, J91.
3 C. Godin and A. Caprani, *Eur. Biophys. J.*, 1996, **25**, 25.
4 Y. X. Huang, Z. J. Wu, J. Mehrishi, B.T. Huang, X.Y. Chen, X. J. Zheng, W. J. Liu and M. Luo, *J. Cell Mol. Med.*, 2011, **15**, 2634.
5 P. N. Sawyer, *Ann. N.Y. Acad. Sci.*, 1983, **416**, 561.
6 P. N. Sawyer, *Ann. N.Y. Acad. Sci*., 1968, **146**, 49.
7 G. M. Delaney, H. P. Bennetto, J. R. Mason, S. D. Roller, J. L. Stirling and C. F. Thurston, *J. Chem. Technol. Biotechnol.*, 1984, **34**, 13.
8 B. H. Kim, H. J. Kim, M. S. Hyun and D. H. Park, *J. Microbiol. Biotechnol*., 1999, **9**, 127.
9 D. R. Bond and D. R. Lovley, *Appl. Environ. Microbiol*., 2003, **69**, 1548.
10 E. Marsili, D. B. Baron, I. D. Shikhare, D. Coursolle, J. A. Gralnick and D. R. Bond, *Proc. Natl. Acad. Sci. USA*, 2008, **105**, 3968.
11 J. Divisek and B. Kastening, *J. Electroanal. Chem.*, 1975, **65**, 603.
12 M. S. Makarov, E. N. Kobzeva, I. V. Vysochin, N. V. Borovkova and V. T. Khvatov, *Bull. Exp. Biol. Med.*, 2014, **156**, 409 (*Byull. Eksp. Biol. Med.*, 2013, **156**, 388).

Received: 10th June 2016; Com. 16/4954